Advance Researches in Civil Engineering
ISSN: 2645-7229, Vol.1, No.3, pages: 58-71

Comparing Semi Active Control of Bridge via Variable Stiffness and Damping Systems and MR Dampers

Fereydoon Amini [1], Sara Zalaghi [1]*

[1] Professor, College of Civil Engineering, Iran University of Science and Technology, Tehran, Iran (famini@iust.ac.ir)*

[1] Research Assistant, College of Civil Engineering, Iran University of Science and Technology, Tehran, Iran

(Date of received: 11/12/2018, Date of accepted: 25/05/2019)

ABSTRACT

Semi active devices can be used to control the responses of a continuous bridge during earthquake excitation. They are capable of offering the adaptability of active devices and stability and reliability of passive devices. This study proposes two semi-active control method protection of bridge using variable stiffness and damping systems and MR dampers. The first method is variable stiffness and damping with eight different (on-off) control schemes which is optimized with genetic algorithm. Genetic algorithm is used to define the parameters of this method. In the second method, an intelligent controller using fuzzy control of MR damper is developed. In particular, a fuzzy logic controller is designed to determine the command voltage of MR dampers. In order to evaluate the effectiveness of the proposed method, the performances of the proposed controllers are compared in numerical study. Results reveal that the developed controllers can effectively control both displacement and acceleration responses of the continuous bridge.

Keywords:

Semi-active devices, MR damper, Variable stiffness, Variable damping, GA algorithm, Fuzzy logic control.

1. Introduction

In recent decades, structural control methods have been developed to three main types of control system: passive, active and semi active system. Semi active control guarantees versatility and the adaptability of active control, and the reliability of the passive control system. Among various types of semi-active controls, one of the practical techniques for simultaneous reduction of total displacement and acceleration during earthquake excitation is seismic isolation [1]. Semi-active suspension is used with a controllable damper, such as fluid damper with variable orifices or magnetorheological (MR) damper [2]. At the same time, variable stiffness concepts have been widely studied for a variety of vibration control applications. Liu et all proposes a Voigot element to achieve variable spring stiffness by using variable damper along with springs connected in series [3]. Magneto-rheological (MR) damper, as semi-active control devices are fluid damper with variable orifices. They can provide large force capacity, high stability robustness and reliability [4]. A wide range of theoretical and experimental studies of a MR damper accepted due to recent rapid practical design related to the development of large scale MR dampers [5]. One of the challenges in the damping force exerted by an MR damper is mainly dependent an appropriate control algorithm to determined the command voltage of the MR damper. Many control algorithms have been proposed to determine input current of a MR damper. However, it isn't easy task because the MR devices are highly none linear to the input voltage [6].

In this study, two semi-active control strategies compensate the effect of any change like displacement in the bridge, are employed to control the behavior the continuous bridge with variable stiffness and MR damper. The first method used variable stiffness and damping with eight different of (on-off) control schemes involving soft and stiff with low and high damping, damping (on-off), stiffness(on-off), and damping and stiffness on-off are investigated. A base isolated structure with variable damping and variable stiffness control were proposed by a few researchers, systems with variable stiffness had a good performance compared to a semi-active system with variable damping and fix stiffness. Thus Liu et all proposed a system with variable stiffness and damping which the stiffness and damping can be easily controlled [3, 7]. In order to achieve reduced response parameters, it is essential to define these design parameters properly. In particular the selection of acceptable parameters has been subjective and Time consuming since it requires a full understanding of system dynamics [8].To overcome this difficulty a genetic algorithm (GA) is applied to the optimal design in this study. The second method is based on fuzzy controller theory for to control semi-active MR dampers. Fuzzy logic controller (FLC) accepted as an effective tool due to advantage such as inherent robustness and ability to deal with nonlinear systems and uncertainties. Fuzzy control systems have a good performance in control problems [9]. In the proposed semi-active fuzzy controller, the built in fuzzy logic characterized by a number of parameters such as member ship functions, fuzzy rules, input/output scaling factors and modulate the input voltage of MR damper. A typical three-span continuous concrete bridge is modeled and investigated with two semi-active proposed controls. VSVD control witch is particularly optimized parameters with GA algorithm, and FLC control method are also adapted for comparison of total displacement. Simulation results demonstrated that the FLC method is more effective than the VSVD control in simultaneously limiting force used by dampers to each pier when the bridge is subjected to earthquake.

Advance Researches in Civil Engineering
ISSN: 2645-7229, Vol.1, No.3, pages: 58-71

2. Control System Design

In this section two semi-active control systems used to control the behavior of the bridge are described and the basic formulation of each method are explained.

2.1. Systems with Variable Characteristics

Systems with variable characteristics are developed to isolate or alleviate vibration because of the uncertainties of excitation such as earthquake in many literatures. The simple idea to develop a system with variable characteristics is to change the stiffness or damping coefficient of the system directly. This variable stiffness or damping systems are widely used in mechanic and civil engineering. The typical systems with variable stiffness or damping are semi-active or active suspension systems [10, 11]. In the paper, the main purpose of using variable stiffness and damping (VSVD) suspension system is to mitigate excitation on the continuous bridge.

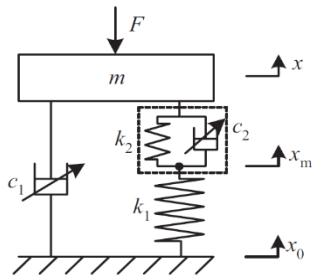

Figure 1. Mechanical configuration of variable stiffness and damping.

In order to illustrate the basic performance of variable stiffness and damping suspension system, a system with single degree of freedom is given in Fig 1. In the model, the suspension system consists of a set of two controllable dampers (corresponding damping coefficients of c_1, c_2) and two springs (corresponding damping stiffness of k_1, k_2) is proposed. Damper 2 and spring 2 comprise a Voiget element. The Voiget element and spring 1 are in series. The stiffness value of the two spring are constant. The aim of using damper 2 is to obtain a suspension system with variable stiffness performance. So the suspension system is a simple modification of a conventional suspension system. The governing equations of the suspension system can be depicted in eq. (1, 2):

$$m\ddot{x} = -k_2(x - x_m) - c_2(\dot{x} - \dot{x}_m) - c_1(\dot{x} - \dot{x}_0) - F \quad (1)$$

$$k_1(x_m - x_0) = k_2(x - x_m) + c_2(\dot{x} - \dot{x}_m) \quad (2)$$

In Figure 1, F is an excitation force, x_0, x and x_m are displacement of base , mass m and the point between the Voiget element and spring 1, respectively[4]. Eight types of control schems shown in Table 1. In Type 4 to Type 8 systems, on-off controlled in damper 1 and 2 as given respectively by eq.(3) and eq.(4). The on-off control algorithm of damper 1 uses the sign of the absolute velocity and the relative velocity. The force f_{d1} generated by damper 1 is:

$$f_{d1} = \begin{cases} -c_{1on}(\dot{x} - \dot{x}_0) & if\ \dot{x}(\dot{x} - \dot{x}_0) \geq 0 \\ -c_{1off}(\dot{x} - \dot{x}_0) & if\ \dot{x}(\dot{x} - \dot{x}_0) < 0 \end{cases} \quad (3)$$

Advance Researches in Civil Engineering
ISSN: 2645-7229, Vol.1, No.3, pages: 58-71

Where the damping coefficient c_1 is equal to c_{1on} in the on-state and c_{1off} in the off-state. The control algorithm in damper 2 uses the sign of $\dot{x}(x - x_0)$. The force f_{d2} exerted by damper 2 is:

$$f_{d2} = \begin{cases} -c_{2on}(\dot{x} - \dot{x_m}) & if\ \dot{x}(x - x_0) \geq 0 \\ -c_{1off}(\dot{x} - \dot{x_m}) & if\ \dot{x}(x - x_0) < 0 \end{cases} \quad (4)$$

The values were used in the numerical calculation: c_{1off} =120π NS/cm, c_{1on} =600 π NS/cm , c_{2off} =69 π NS/cm , c_{2on} = 6930π NS/cm, $k_1 = 1200\pi^2$and $k_2 = k_1/3$. Figure 3(a) shows the schematic diagram of the VSVD control system implementation.

Table 1. Control systems.

	Name	Damper1	Damper2
Type1	Soft system	off	off
Type2	Low damping	off	on
Type3	High damping	on	on
Type4	D on-off(soft)	On-off	off
Type5	D on-off(stiff)	On-off	on
Type6	S on-off(low)	off	on-off
Type7	S on-off(high)	on	on-off
Type8	D+S on-off	On-off	on-off

2.2. MR Damper System

A number of mechanical models for nonlinear damper have recently been proposed by several researchers [4, 5]. In this study, the Bouc-Wen model is used to model the dynamic behavior of the MR damper. A simple mechanical model for the MR damper consisting of a Bouc-Wen element in parallel with a viscous damper is used, as shown in Figure 2.

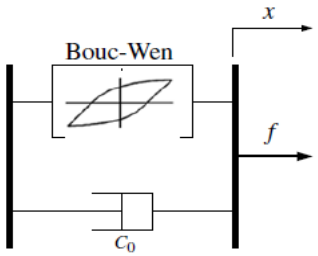

Figure 2. Bouc-Wen model for dynamic behavior of MR damper.

Table 2. Parameters for the MR damper model.

Parameter	Value	Parameter	Value	Parameter	Value
α_a	1.0872× 10^5(N/ cm)	c_{0b}	44.0 $(N/cm/V)$	β	3(cm^{-1})
α_b	4.9616× $10^5(N/cm/V)$	A_m	1.2	γ	3(cm^{-1})
c_{0a}	4.40$(N\,s/cm)$	N	1	η	3(s^{-1})

The equation governing the force f exerted by this model are as follows:

$$f = c_0\dot{x} + \alpha z \quad (5)$$
$$\dot{z} = -\gamma|\dot{x}|z|\dot{z}|^{n-1} - \beta\dot{x}|z|^n + A_m\dot{x} \quad (6)$$

Where x =the displacement of the device, and z =the evolutionary variable the accounts for the history dependence of the response. The Parameters $\gamma.\beta.n.$ and A_m are adjusted to determine the linearity in the unloading and smoothness of the transition from the pre-yield region to the post-yield region. Device model parameters α and c_0 are determined by the dependency on the control voltage u, as follows:

$$\alpha = \alpha(u) = \alpha_a + \alpha_b u \quad (7)$$
$$c_0 = c_0(u) = c_{0a} + c_{0b}u \quad (8)$$

Therefore, the control voltage applied to the current driver in an MR damper continuously modulate the damping force of the MR damper. Moreover, to account for a time-lag in the response of the device to the changes in the command input, the first-order filter dynamics are introduced in to the system as follows:

$$\dot{u} = -\eta(u - v) \quad (9)$$

3. Developments of Control Algorithms

3.1. Genetic Optimal Control Algorithm

As described previously, the design purpose of variable stiffness and damping control with eight schemes the reduction of dynamic responses such as total displacement. An appropriate approach to find the optimum parameters of a VSVD control is to employ computation search techniques. Genetic algorithm (GA) is one of such search techniques based on mechanics of natural genetics. GA searches large spaces without the need of derivative information. Here, single-objective genetic algorithm (SOGA) is used to generate the parameter of VSVD control that specify the force of dampers installed on the bridge. With its powerfull nature, SOGA can efficiently search for effective parameters, additionally it is possible to design a controller that has capability of optimizing displacement response of the bridge using genetic optimization algorithm [8].

In SOGA algorithm, a random population initially is created and then sorted based on non-domination each front. Binary string in GA can represent a candidate of a design variable. GA used binary coding to represent the design variable. After initializing, the fitness of candidates is calculated according to the objective function. The genetic algorithm process is shown in Table 3. The candidates undergo selection process based on the fitness of each individual. In the selection process, the better chromosomes generate higher values than others and place it in the mating pool. Every individual (chromosome) of the design variable (genes) in the population undergoes genetic evolution through crossover and mutation by a defined fitness function. In this study, the roulette wheel selection procedure maps the population in conjunction with the elitist strategy. By using elitist strategy, the best individual in each generation is ensured to be passed to the next generation.

Advance Researches in Civil Engineering
ISSN: 2645-7229, Vol.1, No.3, pages: 58-71

After selection, crossover and mutation, a new population is generated in both GA coding. This new population repeats the same process iteratively until a defined condition.

3.2. Semi- Active Fuzzy Control Strategy

This section explains the semi-active fuzzy control strategy for modulating the MR damper. As shown in the previous section, the magnitudes of the model parameters α and c_0 varies with the input voltage of the MR damper, which lead to the modulation of the damping force of the MR damper. In Fig 3(b) shows a conceptual diagram of a fuzzy control strategy. The semi-active control fuzzy logic strategy takes the response of the MR damper as input information and the input voltage to MR damper as output information. This fuzzy logic is typically consisted of 4 steps: fuzzification, rule-base, inference mechanism, and defuzzification [13].

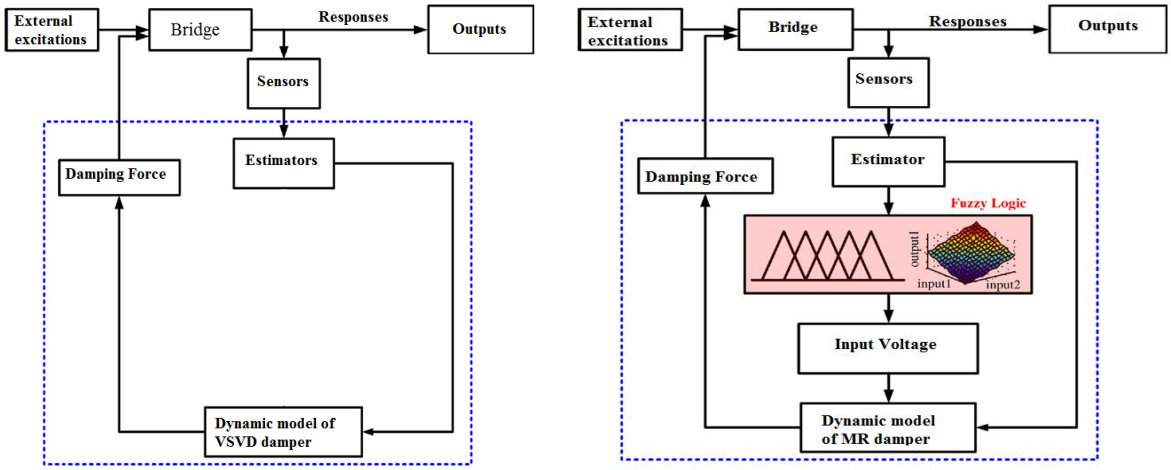

a)Semi-active variable stiffness and variable damping control b)semi-active Fuzzy control

Figure 3. Conceptual diagrams of semi-active control strategies.

In the fuzzification steps, the input information takes the form of a crisp value, which has a physical meaning. To quantify the input information, a fuzzy set is defined using a total of 9 fuzzy variables: NVL, NL, NM, NS, Zero, PS, PM, PL, PVL, where N(negative), P (positive), S(small), M(medium), L(large), V(very) and Zero are used as abbreviations that represent the physical meaning. The rule-base step is created by determining a set of if-premise-then-consequent statement. This fuzzy rule table is specified to represent the relationship between input and output fuzzy variables, where the output varies in proportional to the scale of each given input. The inference mechanism uses the fuzzy rules in the rule-base module to create fuzzified outputs from the fuzzifified inputs [13]. The defuzzification step, the last component of the fuzzy logic, operates on the fuzzified outputs obtained from the inference mechanism. To relate the fuzzified value to the crisp output, a certain inference is required. Similar to the fuzzification process, the fuzzy output variable are defined using a total of 5 output membership functions: Zero, S, M, L, VL. In the dynamic model of the MR damper, the input voltage varies in the range of 0-10 V.

Advance Researches in Civil Engineering
ISSN: 2645-7229, Vol.1, No.3, pages: 58-71

4. Numerical Studies and Discussion

A type of three-span continues concrete bridge as a target used in this study. This continues box Girder Bridge having a total length of 340m with the main span of 160m and two end spans of 90m and the cross sectional details are shown in Fig 4. This continues bridge was modeled using 30 MPa ultimate strength concreate and 190 MN weight of the girder. The maximum allowable displacement is 0.3m this continuous bridge model without controller is used as a model for evaluating the control system. By placing damper devices between the girder and the pier as shown in Fig 5, the damper force generated due to the piston movement will be adjusted independently for each damper based on the control algorithm which is discussed below.

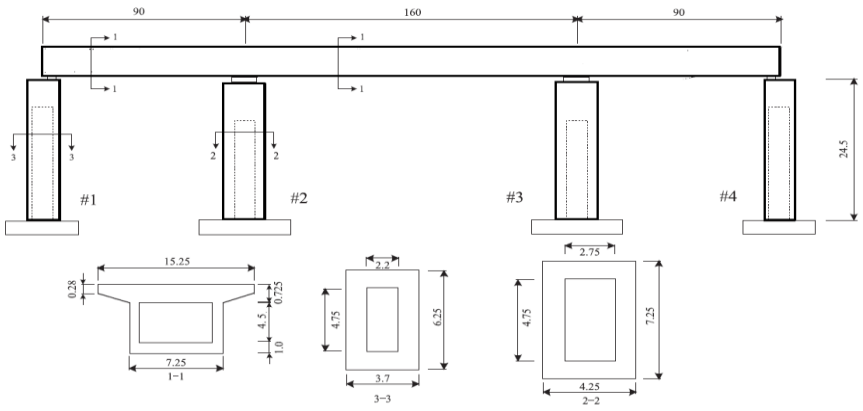

Figure 4. Target bridge model (unit:m).

The numerical simulation of the seismic responses of the benchmark continues bridge are performed within the MATLAB environment through a SIMULINK block. The governing equation of motion for continuous bridge under seismic excitation is:

$$\boldsymbol{M}\ddot{x}(t) + \boldsymbol{C}\dot{x}(t) + \boldsymbol{K}x(t) = -\boldsymbol{M} \cdot \Gamma \cdot \ddot{u}_g(t) + \Lambda \boldsymbol{F}_u(t) \tag{10}$$

Where **M, C** and **K** are mass, damping and stiffness matrices of the bridge, Γ and Λ are the location matrices for ground acceleration $\ddot{u}_g(t)$and control force of the damper$\boldsymbol{F}_u(t)$, the vectors $\ddot{x}(t)$, $\dot{x}(t)$ and $x(t)$ are the acceleration, velocity and displacement, respectively.

Considering Z(t)=$[x(t) \quad \dot{x}(t)]^T$, Eq (10) in state-space form gives:

$$\dot{Z}(t) = AZ(t) + Bu(t) + H\ddot{u}_g(t) \tag{11}$$

Where the state matrix, A, and input matrix B and H are as follows:

$$A=\begin{bmatrix} 0 & I \\ -M^{-1}K & -M^{-1}C \end{bmatrix}, \quad B=\begin{bmatrix} 0 \\ M^{-1}\Lambda \end{bmatrix}, \quad C=\begin{bmatrix} 0 \\ -\Gamma \end{bmatrix} \tag{12}$$

In Eq. (12), I and 0 are identify and Zero matrices respectively.

Advance Researches in Civil Engineering
ISSN: 2645-7229, Vol.1, No.3, pages: 58-71

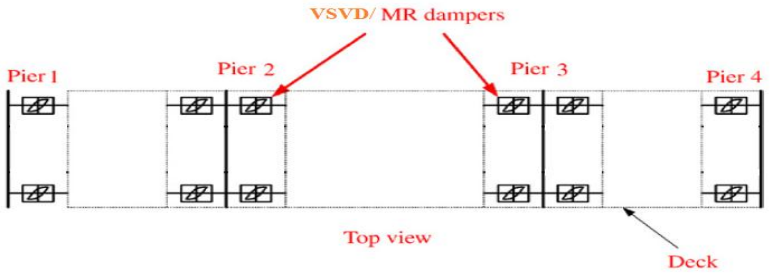

Figure 5. Installation layout of VSVD/MR dampers.

To examine the effectiveness of the bridge by the proposed control algorithms, El Centro ground motion are used as input excitation. The peak ground acceleration is scaled to 0.4g, 0.9g, 1.2g which are corresponding to the medium, strong and extreme level earthquake. Dynamic response analysis is conducted in the longitunal direction of the bridge. In addition, this bridge is assumed to be attached to bed rock, and the effect of soil-structure interaction are neglected. There are eight sets of evaluation criteria which are used in the benchmark problem in structural control to evaluate the performance of the bridge, $J_1$to J_8, as shown in Table 3.

Table 3. Performance indices.

Peak displacement	Peak acceleration	Peak base shear	Peak base over turning moment
$J_1 = \frac{max\|x(t)\|}{max\|\hat{x}(t)\|}$	$J_2 = \frac{max\|a_d(t)\|}{max\|\hat{a}_d(t)\|}$	$J_3 = \frac{max\|V_b(t)\|}{max\|\hat{V}_b(t)\|}$	$J_4 = \frac{max\|M_b(t)\|}{max\|\hat{M}_b(t)\|}$
Peak controlled force	RMS displacement	RMS displacement	Energy dissipated by device
$J_5 = \frac{max\|F(t)\|}{W}$	$J_6 = \frac{max\|\sigma x(t)\|}{max\|\hat{\sigma} x(t)\|}$	$J_7 = \frac{max\|\sigma a_d(t)\|}{max\|\hat{\sigma} a_d(t)\|}$	$J_8 = \frac{\left\{\int_0^T [\dot{x}(t)F(t)]^2 dt\right\}^{1/2}}{\left\{\int_0^T [\dot{x_g}(t)V_b(t)]^2 dt\right\}^{1/2}}$

The maximum base displacement in the controlled bridge normalized by its corresponding value in the uncontrolled bridge is shown by J_1. Similarly acceleration, base shear, base overturning moment in the controlled bridge normalized by corresponding value in the uncontrolled bridge are presented by indices J_2 to J_4, respectively. J_5 represents the maximum control force per device normalized by the total weight of the bridge. Indices J_6 and J_7 determined the root means square of base displacement of the controlled bridge normalized to their values in the uncontrolled respectively. Finally J_8 represent the energy absorbed by the control tool in the controlled bridge normalized by earthquake input energy in the controlled structure. This numerical model is performed in order to investigate the control performance of the variable stiffness and damping (VSVD) control by eight type control system and GA optimization algorithm (VSVD T1 to VSVD T8 and VSVD TGA) which are compared with Fuzzy logic control of MR damper (FLC) and the results are given in Table 4. In fact as shown in Table 3 and Table 4, these comparison results demonstrate that the proposed control strategy is almost quite effective in simultaneously reduce two important structural result responses the maximum displacement and maximum acceleration. Specially among all controller methods, the FLC, VSVD TGA, VSVD T3, T5 are the most effective control methods. The VSVD T3, T7 have the exact performance to the controller developed by VSVD T5, T8 controller respectively.

In three scaled levels of El Centro earthquake, it can be seen that proposed controller significantly reduce J_1 and J_6 , which are performance indices related to the maximum displacement and the value of its RMS, respectively. For example, in comparison with the uncontrolled structures under the El Centro ground motion with PGA of 1.2g the seismic reduction displacement ratio of the bridge are 70.3%, 60.7%, 58.5% and 55.7%, for FLC, VSVD TGA, VSVD T3,5 and VSVD T6,7 respectively. It is clear that the FLC is more effective in reducing the displacement of the bridge than other proposed controller.

Table 4. Performance indices of the bridge subjected to El Centro earthquake.

PGA(g)	Performance indexes	J_1	J_2	J_3	J_4	J_5	J_6	J_7	J_8
	VSVD T1	0.675	0.851	0.712	0.693	1.82E-03	0.798	0.954	0.33
	VSVD T2	0.526	0.885	0.652	0.541	3.59E-03	0.587	0.933	0.58
	VSVD T3,5	0.415	0.628	0.371	0.289	4.90E-03	0.475	0.761	0.89
	VSVD T4	0.555	0.856	0.532	0.471	4.23E-03	0.59	0.781	0.84
1.2	VSVD T6	0.509	1.062	0.672	0.635	3.38E-03	0.602	0.947	0.57
	VSVD T7,8	0.443	0.763	0.391	0.341	5.46E-03	0.468	0.773	0.81
	VSVD TGA	0.393	0.671	0.352	0.314	4.68E-03	0.474	0.769	0.8
	FLC	0.297	0.643	0.282	0.267	6.36E-03	0.354	0.652	0.88
	VSVD T1	0.704	0.998	0.682	0.651	1.22E-03	0.788	0.949	0.34
	VSVD T2	0.558	1.008	0.647	0.553	2.65E-03	0.596	0.966	0.61
	VSVD T3,5	0.443	0.827	0.348	0.311	4.30E-03	0.475	0.779	0.92
	VSVD T4	0.559	0.838	0.492	0.461	3.74E-03	0.594	0.839	0.86
0.9	VSVD T6	0.552	1.002	0.685	0.627	2.46E-03	0.613	0.934	0.63
	VSVD T7,8	0.417	0.718	0.392	0.347	4.23E-03	0.463	0.758	0.83
	VSVD TGA	0.41	0.992	0.421	0.391	3.51E-03	0.48	0.786	0.61
	FLC	0.161	0.429	0.261	0.231	5.93E-03	0.373	0.632	0.81
	VSVD T1	0.736	1.011	0.651	0.637	5.87E-04	0.599	0.947	0.4
	VSVD T2	0.528	0.862	0.727	0.699	1.17E-03	0.593	0.934	0.63
	VSVD T3,5	0.422	0.652	0.451	0.438	1.73E-03	0.468	0.754	0.79
	VSVD T4	0.551	0.808	0.422	0.417	1.54E-03	0.581	0.785	0.85
0.4	VSVD T6	0.538	0.869	0.525	0.505	1.15E-03	0.6	0.947	0.56
	VSVD T7,8	0.451	0.705	0.418	0.398	1.86E-03	0.469	0.754	0.83
	VSVD TGA	0.447	0.935	0.432	0.407	1.85E-03	0.472	0.762	0.8
	FLC	0.012	0.357	0.287	0.248	4.41E-03	0.374	0.678	0.1

Also considering indices J_2 and J_7 , it can be seen that decreases in maximum acceleration in the most cases and the value of its RMS. For example, in comparison with the uncontrolled bridge FLC resulted in 35.7%, 57.1%, 64.3% decrees in peak acceleration for 1.2g, 0.9g and 0.4g scaled level of El Centro earthquake respectively, considering these levels of earthquake, in the most case by about 10-20%. It is clear that the FLC performs better in reduction of the maximum bridge acceleration. For some controller however, the results indicate that any attempt to reduce the maximum displacement would leads to increasing structures maximum accelerations in comparison with the uncontrolled case. For the El Centro ground motion with a PGA of 1.2g, VSVD T6 lead to increase of 6.2% in terms of maximum acceleration; similarly these increase are

Advance Researches in Civil Engineering
ISSN: 2645-7229, Vol.1, No.3, pages: 58-71

0.8%, 0.2% for VSVD T2 and VSVD T6 respectively with a PGA of 0.9g and 1.1% for VSVD T1 with a PGA of 0.4g. Considering J_1 and J_6 which are performance indices related to the maximum displacement and it can be the value of its RMS.

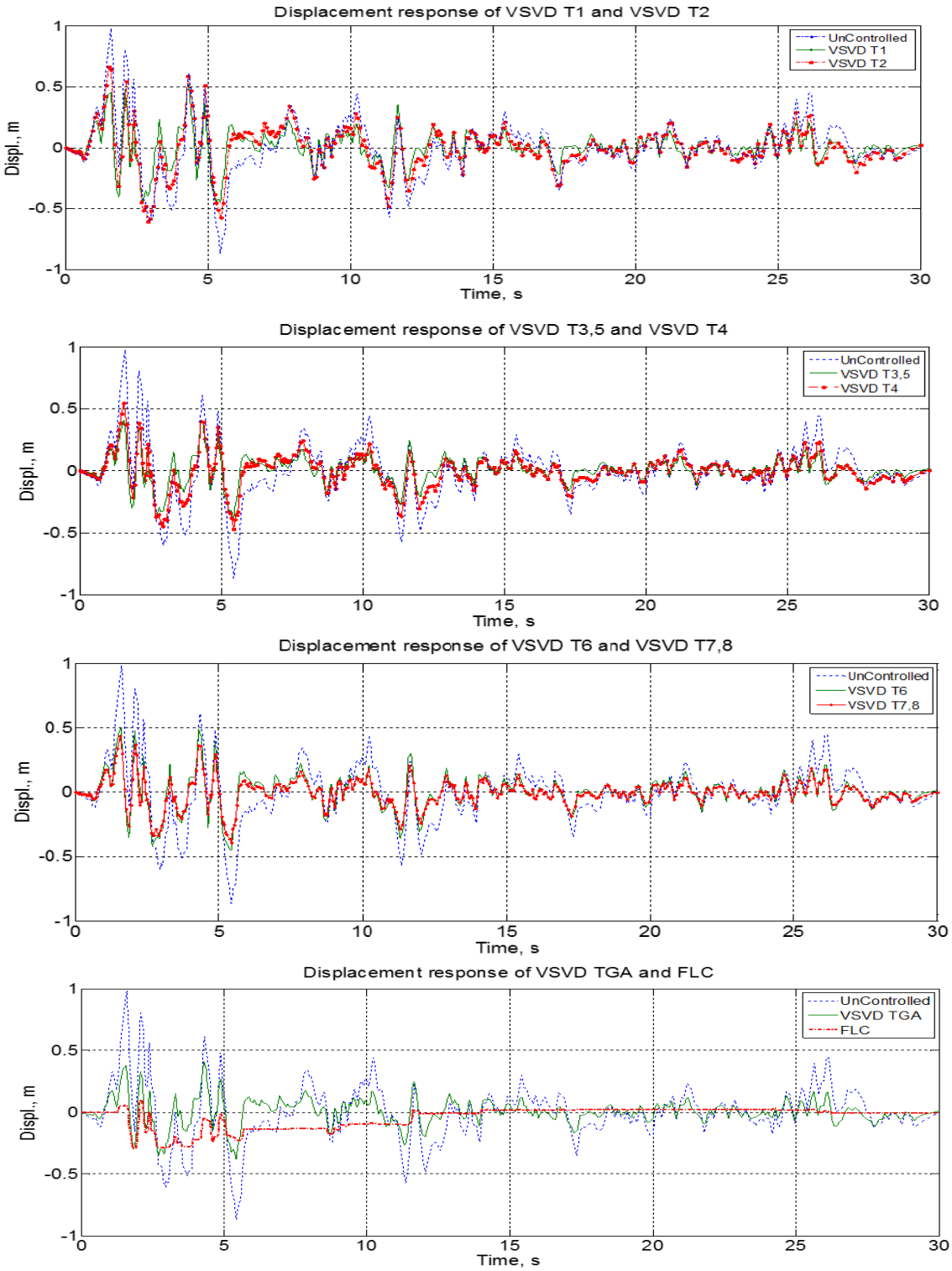

Figure 6. Displacement time histories of the side pier under El Centro earthquake with a PGA 1.2g.

Advance Researches in Civil Engineering
ISSN: 2645-7229, Vol.1, No.3, pages: 58-71

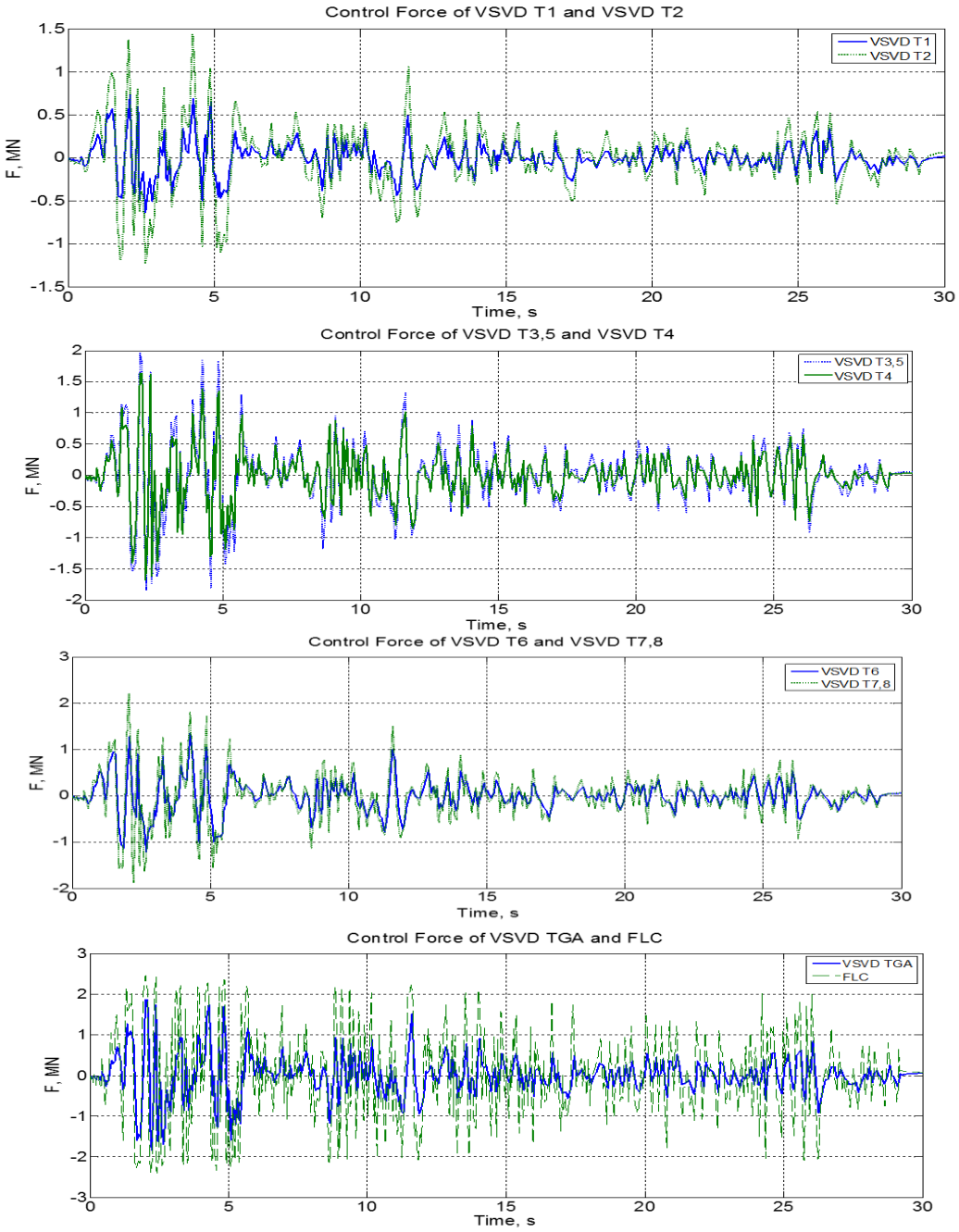

Figure 7. Control Force time histories of the side pier under El Centro earthquake with a PGA 1.2 g.

As seen that the FLC controller is able to significantly reduce the maximum displacement and the value of its RMS. Furthermore by comparing the results provided by the FLC controller with those given by other controller techniques in reduction of performance indices J_2 and J_7 , the maximum acceleration be concluded that the proposed controller provide the best performance. Considering the values of performance indices J_3 and J_4 which are related to the base shear and overturning moment respectively, it can be seen that the best result are obtained by the proposed controller in the three scaled level of El Centro earthquake. Even, for other evaluation criteria J_5, J_8

the proposed system still shows very competent control performance. Nonetheless, using J_5 evaluation criteria all of the proposed controller methods described above are the same range based on the maximum control force.

The value of indice J_8 indicate that the performance of the proposed controller can be compared in terms of dissipated energy normalized by input excitation energy. The VSVD T3.5 controller perform better than other control strategies in term of dissipation of input excitation energy in three scaled levels of El Centro earthquake. It should be noted the FLC, VSVD T3.5 and VSVD TGA controllers by comparison in term of dissipated energy and maximum control force are almost the same range, while FLC controller provides a better performance in reduction in maximum displacement and maximum acceleration.

Considering three scaled level of El Centro earthquake which are corresponding to the medium, strong and extreme level earthquake. Fig 6 shows the displacement time histories of proposed controllers in side piers under the extreme level with a PGA of 1.2 g. It is evident that control efficiencies of both VSVD TGA and FLC on the piers of continues bridge are generally higher than the other proposed controller. Fig 7 shows the time histories of controlled force generated in side pier of proposed controllers under the extreme level with a PGA of 1.2 g. It is indicated the same range of control force entered to continues bridge. The time history of the command voltage provided by the FLC control is presented in Figure 8. It can be seen that the maximum command voltage is '10 V' during real-time control.

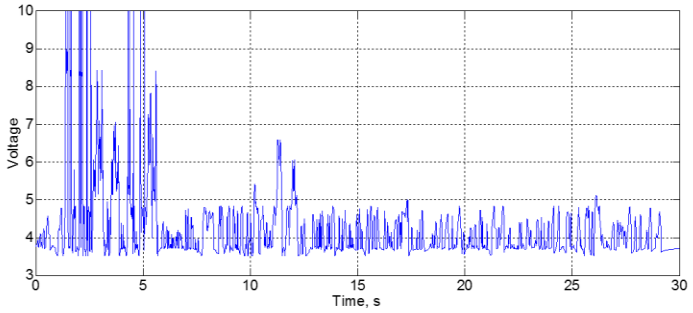

Figure 8. Time history of command voltage.

Finally, in order to assess the stability of sensitivity of the proposed controllers with regard to uncertainties in seismic excitation, simulations of the bridge under three scaled level of El Centro earthquake. To investigate the sensitivity of the proposed controller uncertainties, an uncertainty of $\pm 10\%$ in the stiffness is considered. For three important performance indices i.e. J_1, J_2 and J_5 , the performance of the proposed controller is evaluated in Table 5. It can be seen that developed controller is evaluated in Table 5 satisfactorily suppress the response of the bridge under three scaled level of El Centro earthquake. In particular, FLC controller is maintains appropriate performance in dealing with model uncertainties. This means that is not sensitive to modelling errors and show an invariant performance against model uncertainties.

Table 5. Performance indices of the bridge subjected to El Centro earthquake.

Performance index		J_1			J_2			J_5		
PGA(g)	With uncertainty	-10%	0%	10%	-10%	0%	10%	-10%	0%	10%
1.2	VSVD T1	0.683	0.675	0.667	0.904	0.851	0.993	1.77E-03	1.82E-03	1.96E-03
	VSVD T2	0.499	0.526	0.513	0.982	0.885	1.023	3.47E-03	3.59E-03	3.50E-03
	VSVD T3,5	0.41	0.415	0.444	0.898	0.628	0.915	4.71E-03	4.90E-03	5.52E-03
	VSVD T4	0.543	0.555	0.529	0.649	0.856	0.669	4.65E-03	4.23E-03	5.03E-03
	VSVD T6	0.543	0.509	0.533	0.836	1.062	1.043	3.41E-03	3.38E-03	3.39E-03
	VSVD T7,8	0.451	0.443	0.427	0.693	0.763	0.956	5.51E-03	5.46E-03	5.53E-03
	VSVD TGA	0.419	0.393	0.443	0.837	0.671	0.982	5.65E-03	4.68E-03	5.37E-03
	FLC	0.297	0.297	0.297	0.649	0.643	0.654	6.36E-03	6.36E-03	6.36E-03
0.9	VSVD T1	0.693	0.704	0.714	0.982	0.998	0.987	1.27E-03	1.22E-03	1.25E-03
	VSVD T2	0.565	0.558	0.524	0.949	1.008	1.003	2.54E-03	2.65E-03	2.54E-03
	VSVD T3,5	0.423	0.443	0.436	0.822	0.827	0.736	3.59E-03	4.30E-03	4.13E-03
	VSVD T4	0.691	0.559	0.546	0.859	0.838	0.841	3.31E-03	3.74E-03	3.64E-03
	VSVD T6	0.544	0.552	0.544	0.983	1.002	1.022	2.55E-03	2.46E-03	2.51E-03
	VSVD T7,8	0.453	0.417	0.446	0.865	0.718	0.817	3.85E-03	4.23E-03	4.08E-03
	VSVD TGA	0.427	0.41	0.433	0.716	0.992	0.711	3.63E-03	3.51E-03	4.05E-03
	FLC	0.199	0.161	0.161	0.475	0.429	0.482	5.93E-03	5.93E-03	5.93E-03
0.4	VSVD T1	0.704	0.736	0.728	0.97	1.011	0.859	6.35E-04	5.87E-04	6.33E-04
	VSVD T2	0.516	0.528	0.533	0.967	0.862	0.901	1.18E-03	1.17E-03	1.08E-03
	VSVD T3,5	0.401	0.422	0.436	0.835	0.652	0.616	1.91E-03	1.73E-03	1.81E-03
	VSVD T4	0.554	0.551	0.537	0.964	0.808	0.552	1.62E-03	1.54E-03	1.51E-03
	VSVD T6	0.542	0.538	0.556	0.982	0.869	1.032	1.09E-03	1.15E-03	1.09E-03
	VSVD T7,8	0.432	0.451	0.445	0.717	0.705	0.743	1.87E-03	1.86E-03	1.79E-03
	VSVD TGA	0.447	0.447	0.408	0.798	0.935	0.658	1.84E-03	1.85E-03	1.59E-03
	FLC	0.012	0.012	0.012	0.312	0.357	0.347	4.39E-03	4.41E-03	4.39E-03

5. Conclusions and Discussions

Tow semi-active control methods are proposed in this study to control the performance of continues bridge equipped with variable stiffness and damping and MR dampers. The first method is variable stiffness and damping with eight different control schemes which is optimized with genetic algorithm. Genetic algorithm is used to define the parameters of VSVD damper. In the second approach, an intelligent controller using fuzzy control of MR damper is developed. By comparing the performance of the proposed controller, it was revealed that the proposed controller almost can significantly decrease the peak displacement while simultaneously reducing maximum absolute acceleration. The effect of variable stiffness and damping systems on reduce responses structures are obvious, especially VSVD TGA is generally have more advantage than the other variable characteristics controllers. Also, in comparison FLC method with variable characteristic methods depicted the FLC controller demonstrated a better performance in reduction displacement and acceleration. Moreover, proposed controller provide acceptable responses in terms RMS of displacement and peak acceleration. Finally, the sensitivity of the proposed controllers was assessed by considering a stiffness uncertainty of $\pm 10\%$ and it was shown that the proposed controller, in particularly FLC controller could provide an acceptable performance in dealing with the given method uncertainty.

The simulation results demonstrate that the fuzzy controlled MR damper system is quiet effective in reducing the responses of continues bridge to a medium, strong and extreme level earthquake.

6. References

[1]-Housner, G. W., Bergman, L. A., Caughey, T. K., Chassiakos, A. G., Claus, R. O. and Masri, S. F., 1997, **Structural control: past, present, and future**, Journal of Engineering Mechanics,123(9), 897-971.

[2]- Oh, S. K., Yoon, Y. H., Krishna, A. B., 2007, **A study on the performance characteristics of variable valve for reverse continuous damper**, World Academic Science, Engineering Technology, 32, 123–128.

[3]- liu, Y., Matsuhisa, H., Utsuno, H., 2008, **Semi-active vibration isolation system with variable stiffness and damping control**, Journal of sound and vibration, 313, 16-28.

[4]- Dyke, S. J., Spencer, B. F., Sain, M. K., Carlson, J. D., 1996, **Modelling and control of magnetorheogical dampers for seismic response reduction**, Smart Material Structure, 5, 565-575.

[5]- Sodeyama, H., Sunakoda, K., Suzuki, K., Carlson, J. D., Spencer, Jr. B. F., 2001, **Development of large capacity semi active vibration control device using magnetorheological fluid**, Seismic Engineering ASME PVP, 428(2), 109-114.

[6]-Yi, F., Dyke, S. J., Caicedo, J. M., Carlson, J. D., 2001, **experimental verification of multinput seismic control strategies for smart dampers**, Journal of Engineering Mechanics, 127(11), 1152-1164.

[7]- liu, Y., Matsuhisa, H., Utsuno, H. and Park, J. G., 2005, **Vibration isolation by a variable Stiffness and Damping System**, International Journal Society of Mechanical Engineering, 48(2), 305-310.

[8]- Marano, G. C., Quaranta, G., and Monti, G., 2011, **Modified genetic algorithm for the dynamic identification of structural systems using incomplete measurements**, Computing-Aided Civil Infrastructure Engineering, 26(2), 92-110.

[9]- Lee, C. C., 1995, **Fuzzy logic in control system: fuzzy logic controller part I and part II**., IEEE Transaction System Man, and Cybernetics, 20, 404-418.

[10]- Cronje, J. M, Stephan, P., and Theron, N. J., 2005, **Development of a variable stiffness and damping runnable vibration isolator**, Journal Vibrate control, 11(3), 381-396.

[11]- Gonca, V., and Shavab, J., 2010, **Design of elastomeric shock absorbers with variable stiffness**, Journal Vibroengineering, 12(3), 347-354.

[12]- Yoshida, O., and Dyke, S. J., **Seismic control of a nonlinear benchmark building using smart dampers**, Journal of Engineering Mechanics, 130(4), 386-392.

[13]- Park, K. S., Koh, M. H., and Seo, C. W., 2004, **Independent model space fuzzy control of earthquake-excited structures**, Engineering Structures, 26, 279-289.